Transport due to Electromagnetic Turbulence in Externally Heated Plasma

A. Ishizawa and N. Nakajima

National Institute for Fusion Science, Toki, Gifu, 509-5929, Japan

e-mail contact of main author : ishizawa@nifs.ac.jp

Abstract. Turbulent transport caused by multi-scale interactions among electromagnetic micro-turbulence, tearing mode, and zonal flow is investigated by numerically solving a reduced set of two-fluid equations. A new three-dimensional numerical simulation of transport phenomena in an open system controlled by external heat source and sink is proposed by virtue of self-consistent calculation of the multi-scale interactions. When tearing mode appears in a quasi-equilibrium including micro-turbulence and zonal flow, the energy spectrum of micro-turbulence is changed so that the energy of the dominant toroidal mode representing micro-turbulence is reduced and the energy of small toroidal mode including tearing mode increases. At the same time the ion temperature profile is flattened and thermal diffusion coefficient increases around the magnetic islands due to tearing mode. The zonal flow shear becomes strong around the magnetic island.

1. Introduction

Micro-instabilities cause micro-turbulence and strongly enhance heat and particle transport [1]. In high beta toroidal plasmas micro-turbulence involves electromagnetic fluctuation, in addition, macro-MHD instability can be destabilized. Macro-MHD instabilities cause global deformation of plasma, especially, tearing modes violate magnetic surfaces and significantly degrade plasma confinement. Micro-turbulence and macro-MHD instability appear in the plasma confinement simultaneously. For instance, a macro-MHD activity is observed in the reversed shear tokamak plasma, when a transport barrier, which is related to zonal flow and micro-turbulence, is observed [2], and fluctuation due to micro-turbulence is observed in Large Helical Device which usually exhibits macro-MHD instability due to high beta of plasma [3]. Mutual interaction between micro-turbulence and macro-MHD instability is a multi-scale interaction and can cause a different thermal transport compared to the one by each of them.

Multi-scale interactions in magnetically confined plasmas are investigated analytically and numerically [4]-[12]. The interaction between micro-turbulence and zonal flow is a typical multi-scale interaction [4] because toroidal and poloidal mode numbers of micro-instabilities are much larger than one, while these numbers are zero for zonal flow. There are another multi-scale interaction between different instabilities which are independent in linear evolution when their free energies are different, for instance, there are interactions between micro-instability due to pressure gradient and macro-MHD instability that is caused by current density gradient and has low toroidal and poloidal mode numbers.

In the previous study we considered a situation that a current driven macro-MHD instability arises in a quasi-equilibrium including micro-turbulence and zonal flow. This is because a macro-MHD instability is destabilized when there arises one or more resonant q surfaces where the safety factor q is equal to a small rational number, while micro-instabilities can arise even if there is no integer q surfaces. Thus, micro-turbulence almost always exists before destabilization of macro-MHD instability. In order to examine this situation we carried out a three-dimensional numerical simulation of a reduced set of two-fluid equations and investigated mutual interaction between micro-turbulence and macro-MHD mode (double tearing

mode) [9, 10]. In the simulation micro-instabilities (kinetic ballooning mode) are destabilized at first, and then turbulent state is formed. We found that the excitation of macro-mode by the micro-turbulence is different from macro-MHD instability because the spatial profile of the former is significantly different from the spatial profile of double tearing mode. The energy transfer from micro-turbulence to macro-mode is similar to the energy transfer from micro-turbulence to zonal flow [10]. The macro-mode is a part of turbulence in the turbulent state. After a certain period of time, then, the induced macro-mode by the turbulence becomes eigen function of double tearing mode and grows up with magnetic reconnection, in the case that the equilibrium has free energy of macro-MHD instability such as a current density gradient [9]. When the free energy is small the double tearing mode saturates, and then we have a new quasi-equilibrium including not only the micro-turbulence and zonal flow but magnetic islands [11]. The magnetic reconnection of double tearing mode is caused by non-ideal effect due to turbulent mixing of magnetic flux at the resonant surfaces [11]. The effect of zonal flow produced by micro-turbulence on the stability of double tearing mode is not clear [12], while the zonal flow shear is suppressed by the appearance of double tearing mode as implied in Ref. [9].

In this paper we study effects of coexistence of micro-turbulence with macro-MHD instability on turbulent thermal transport in externally heated plasma. Self-consistent calculation of the mutual interaction is carried out by numerically solving a reduced set of two-fluid equations. We examine thermal transport due to electromagnetic turbulence by comparing before arising macro-MHD instability in an equilibrium including micro-turbulence and afters. This analysis of heat transport in the presence of macro-MHD is motivated by experimental results showing dependence between the formation of transport barrier and the integer q surfaces[13].

2. Simulation model

We carry out three-dimensional numerical simulations of a reduced set of two-fluid equations that extends the standard reduced two-fluid equations[14] by including temperature gradient effects[15, 16, 9]. The equations are

$$
\begin{aligned}
n_{eq}\frac{d\nabla_\perp^2\Phi}{dt} &= -\nabla_\parallel J - K[p] + \tilde{a}\nabla_\perp\cdot[\nabla_\perp\Phi, p_i] + \mu_Q\nabla_\perp^2\nabla_\perp^2\Phi, && (1)\\
\frac{dn}{dt} &= -n_{eq}\nabla_\parallel v_{e\parallel} + K[n_{eq}\Phi - p_e] + \mu_n\nabla_\perp^2 n, && (2)\\
n_{eq}\frac{dv_\parallel}{dt} &= -\nabla_\parallel p + \mu_v\nabla_\perp^2 v_\parallel, && (3)\\
\beta\frac{\partial\psi}{\partial t} &= -\nabla_\parallel\Phi + \frac{1}{n_{eq}}\nabla_\parallel p_e + \eta_L v_{e\parallel} + \eta J, && (4)\\
\frac{dT_i}{dt} &= -(\Gamma-1)(T_{eq}\nabla_\parallel v_\parallel + \kappa_L T_i) \\
&\quad + T_{eq}K[(\Gamma-1)(\Phi + T_i + T_{eq}n/n_{eq}) + \Gamma T_i] + \mu_T\nabla_\perp^2 T_i, && (5)
\end{aligned}
$$

where $df/dt = \partial f/\partial t + \tilde{a}[\Phi, f]$, $\nabla_\parallel f = \epsilon\partial f/\partial\zeta - \beta\tilde{a}[\psi, f]$, $K[f] = 2\epsilon[r\cos\theta, f]$, $J = \nabla_\perp^2\psi$, $\psi = \psi_{eq} + \tilde{\psi}/\tilde{a}$, $\Phi = \tilde{\Phi}/\tilde{a}$, $n = n_{eq} + \tilde{n}/\tilde{a}$, $T_i = T_{eq} + \tilde{T}_i/\tilde{a}$, $T_e = \tau T_{eq}$, $p_i = n_{eq}T_{eq} + T_{eq}\tilde{n}/\tilde{a} + n_{eq}\tilde{T}_i/\tilde{a}$, $p_e = \tau n_{eq}T_{eq} + \tau T_{eq}\tilde{n}/\tilde{a}$, $p = p_i + p_e$, $v_{e\parallel} = v_\parallel + J/n_{eq}$, $\tilde{a} = a/\rho_i$, $\eta_L = \sqrt{\frac{\pi}{2}\tau\frac{m_e}{m_i}}|\nabla_\parallel|$,

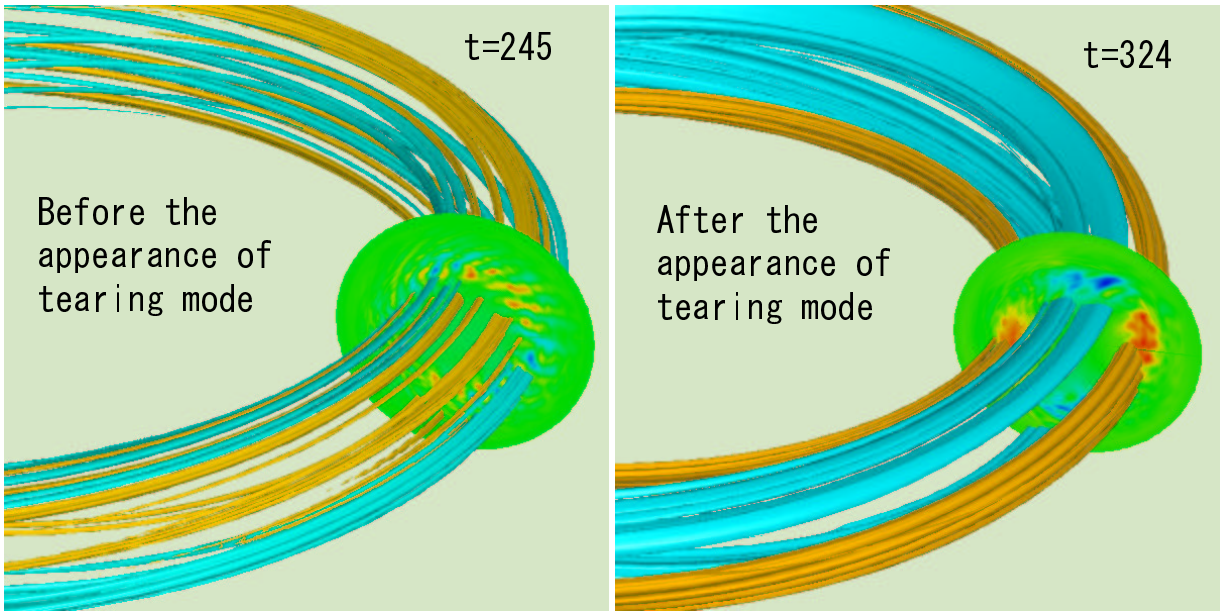

FIG. 1: *Three-dimensional color-contour of electrostatic potential. The quasi-steady state including electromagnetic turbulence is formed at* $t = 245$. *After the appearance of tearing mode the spatial structure of turbulence is altered at* $t = 324$.

$\kappa_L = \sqrt{\frac{8T_{eq}}{\pi}}|\nabla_\parallel|$. In these equations n, $v_\parallel$, Φ, ψ, T_i, ρ_i, $\epsilon = a/R$, R, and a are the electron density, the parallel ion velocity, the electrostatic potential, the flux function, the ion temperature, Larmor radius, the inverse of aspect ratio, the major radius, and the minor radius, respectively. The normalizations are $(tv_{ti}/a, r/\rho_i, \rho_i\nabla_\perp, a\nabla_\parallel, e\Phi/T_0, \psi/\beta B_0\rho_i, n/n_0, T/T_0, v_\parallel/v_{ti})$ $\rightarrow (t, r, \nabla_\perp, \nabla_\parallel, \Phi, \psi, n, T, v_\parallel)$. In the numerical calculations we employ 128 toroidal modes and 256 poloidal modes that distribute within $1 \leq m/n \leq q(r/a = 0.9)$, and 256 uniform grid points in the radial direction, where m and n are poloidal and toroidal mode numbers. We set $\epsilon = 0.25$, $\rho_i/a = 1/80$, $\tau = 1$, the artificial dissipations $\mu_Q = \mu_n = \mu_v = \mu_T = m^4 10^{-7}$, and the normalized resistivity $\eta = 4 \times 10^{-4}$ which corresponds to $S = 1.6 \times 10^6$. We assume that the plasma is surrounded by a perfectly conducting wall.

We describe the initial equilibrium of numerical simulation here. We consider a normal shear q-profile, $q = q_0\{1 + (r/\tilde{a})^{2p}[(q_a/q_0)^p - 1]\}^{1/p}$, where $q_0 = 1.7$, $q_a = 4$, and $p = 4$, that has a $q = 2$ resonant surface at $r/\tilde{a} = 0.65$. The density profile is $n_{eq} = 0.8 + 0.2\exp(-4(r/\tilde{a})^2)$, and the temperature profile is $T_{eq} = 0.8 - 0.2\tanh[(r/\tilde{a} - 0.7)/0.2]$. Kinetic ballooning modes[17], i.e. micro-instability, are unstable and a tearing mode[18], i.e. macro-MHD instability, is also unstable for the initial equilibrium.

3. Nonlinear evolution in external heating

We consider a situation that turbulent plasma is externally heated because micro-turbulence exists before heating the plasma additionally in many torus plasma experiments. For such purpose, first, we calculate time evolution of micro-instabilities for a fixed temperature profile and obtain a quasi-equilibrium that includes the micro-turbulence. This calculation is similar to our

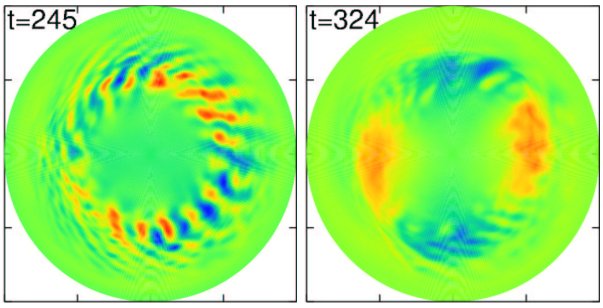

FIG. 2: *Color-contour of electrostatic potential on the same poloidal cross section. The quasi-equilibrium including micro-turbulence is formed at* $t = 245$. *The coexistence of micro-turbulence with tearing mode is established at* $t = 324$.

previous one that shows production of small (m, n) mode by micro-turbulence [9, 10] and is described in Sec. 3.1. Next we do not fix the temperature profile and add heat into the quasi-equilibrium, and then we restart the numerical simulation. We choose the appropriate heating that makes up for the turbulent heat transport so that the temperature profile is sustained. This is described in Sec. 3.2. When we have macro-MHD instability we can have flattening of profile even if we try to sustain the profile by the appropriate heating. This is shown in Secs. 3.3 and 3.4.

3.1. Formation of quasi-equilibrium and production of small (m,n) mode by turbulence

The kinetic ballooning modes are more unstable than the tearing mode for the initial equilibrium, and thus kinetic ballooning modes dominate in the early evolution and make the system be turbulent. The three-dimensional color-contour of electrostatic potential shows a ballooning structure, which is fat at the outer side of torus and is thin at the inner side at $t = 245$ in Fig. 1. The turbulence is strong at the bad curvature region as shown in the frames with $t = 245$ of electrostatic potential profile in Fig. 2. The zonal flow is produced by the turbulence and regulates the amplitude of turbulence by shearing radial profile of turbulence as shown in the frames with $t = 245$ in Fig. 2.

Here we present the time evolution of magnetic energy, $E_M(n)$, and kinetic energy $E_K(n)$ for each toroidal mode number n in Fig. 3. The kinetic ballooning modes, $7 \leq n \leq 20$, increase at first, and the $n = 1$ mode (blue thick line) that indicates macro-mode also increases because of nonlinear mode coupling with the kinetic ballooning modes. Then, all modes saturate and zonal flow, which is indicated by the $n = 0$ mode of kinetic energy (red thick line), regulates the level of turbulence. At this time the $(m, n) = (2, 1)$ mode is a part of turbulence and the helical flux of $m/n = 2$ does not show magnetic islands in the frame of $t = 245$ of Fig. 4. To be precise, electromagnetic perturbation of micro-turbulence violates magnetic surfaces around $q = 2$ rational surface at $t = 245$ as shown by Poincare map of magnetic field lines in Fig. 4. Hence, the growth of $(m, n) = (2, 1)$ mode by the nonlinear mode coupling with the turbulence is not the growth of tearing mode as mentioned in Ref. [9].

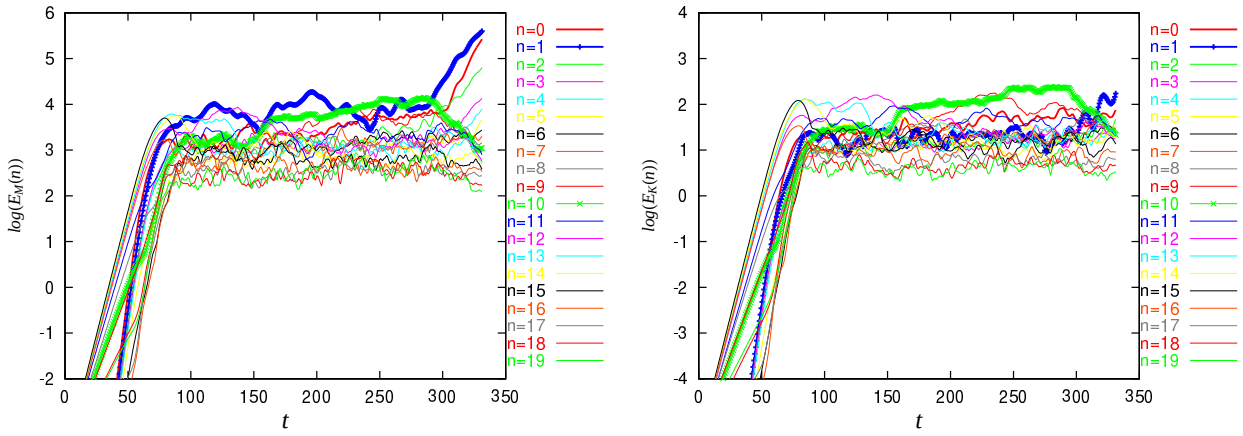

FIG. 3: *Time evolutions of magnetic energy (left) and kinetic energy (right) for each toroidal mode number n. Evolution of macro-MHD mode (tearing mode for $t > 290$) is indicated by $n = 1$ mode and micro-instability (kinetic ballooning mode) is indicated by $7 \leq n \leq 20$ mode. The amplitude of $n = 10$ mode decreases after the tearing mode grows.*

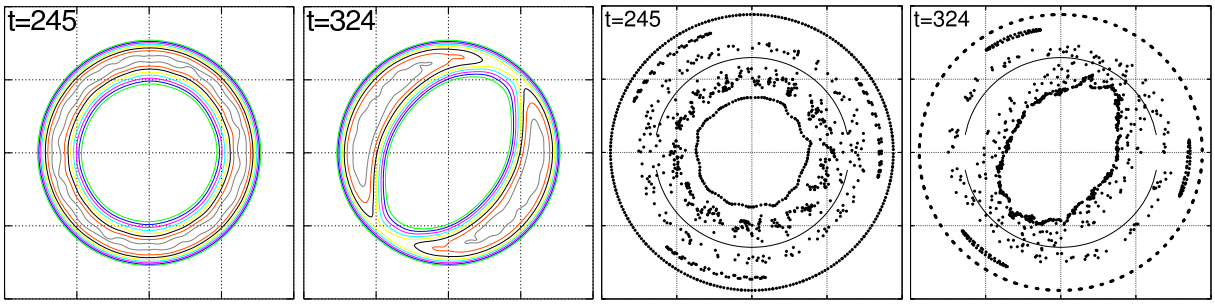

FIG. 4: *Equi-contour of helical flux function of $m/n = 2$ on a poloidal cross section (left two frames). Poincare map of magnetic field lines (right two frames, where bold line indicates $q = 2$ rational surface of the initial equilibrium). There is no magnetic islands at $t = 245$. Magnetic islands with $(m, n) = (2, 1)$ appear at $t = 324$.*

3.2. External heating

In the previous section we have shown the formation of a quasi-equilibrium including micro-turbulence and zonal flow. Here, we do not fix the temperature profile of the quasi-equilibrium from $t = 151$ and externally add heat source and heat sink to the plasma so that the temperature profile does not change. We have obtained the numerical data of heat flux from the simulation before $t = 151$. Based on the data we evaluate heat source and heat sink that are required to sustain the original temperature profile. Then, we restart our simulation and examine the subsequent evolution. If we do not heat the plasma the turbulence makes temperature profile flatten, and then the amplitude of turbulence decreases. We choose appropriate heating so that the temperature profile remains when the quasi-equilibrium is stable against macro-MHD instabilities. In this unstable case, however, a tearing mode arises at $q = 2$ resonant surface and it can change the profile.

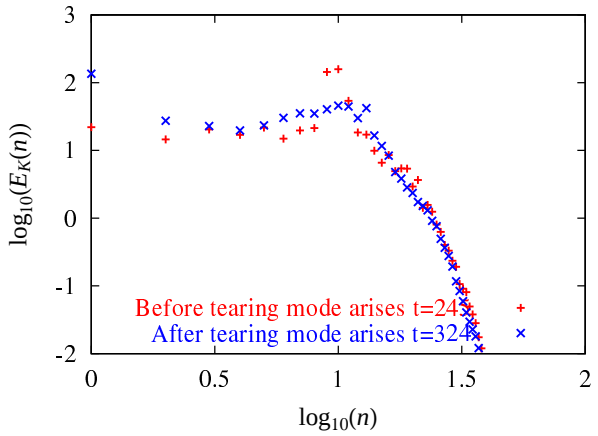

FIG. 5: *Energy spectrum kinetic energy at $t = 245$ and 324. The dominant mode of micro-turbulence, $n = 9$ and 10 decreases after the appearance of tearing mode.*

3.3. Appearance of macro-MHD instability (tearing mode)

In the quasi-equilibrium which continues until $t = 290$, the $(m, n) = (2, 1)$ mode is not a tearing mode but a part of the turbulence. Then, the magnetic energy of $n = 1$ mode starts to grow at $t = 290$ in Fig. 3. This macro-scale instability is the tearing mode because the helical flux of $m/n = 2$ represents magnetic islands in the frame of $t = 324$ of Fig. 4. Poincare map of magnetic field lines also shows the appearance of large $m = 2$ structure around $q = 2$ rational surface at $t = 324$ in Fig. 4. The ballooning structure of three-dimensional color contour changes its shape into the $(m, n) = (2, 1)$ structure that is fat at both the outer and the inner sides of torus in Fig. 1. Figure 5 shows energy spectrum before and after the appearance of tearing mode. The dominant toroidal modes of turbulence are $n = 9$ and 10, and the amplitudes of these modes are reduced after the tearing mode arises. On the other hand the energy of low toroidal mode less than 10 increases. Hence, the energy spectrum of turbulence is changed by the appearance of tearing mode.

3.4. Transport enhancement by the appearance of tearing mode

Figure 6 (a) shows ion temperature profiles before and after the presence of tearing mode. After the tearing mode appears the flattening of ion temperature profile occurs around the resonant surface of $q = 2$, $r_s/\tilde{a} = 0.65$. Figure 6 (b) shows the heat diffusivity χ_i profiles and zonal flow profiles before the appearance of tearing mode and afters. The heat diffusivity increases around the resonant surface of $q = 2$. We think mechanism of transport enhancement is that the tearing mode produces not only coherent magnetic islands but also macro-scale convective cell flow. The large scale flow of tearing mode cooperates with small-scale turbulent flow and strongly enhances the convection of heat.

The zonal flow profile changes its shape after the presence of tearing mode as shown in Fig. 6 (b). After the presence of tearing mode the zonal flow shear becomes strong around the magnetic islands that is located at $r_s/\tilde{a} = 0.65$. Figure 7 shows time evolution of zonal flow profile. After $t = 300$ the flow profile changes around $r_s/\tilde{a} = 0.65$ where magnetic island appears. The zonal flow shear is expected to be strong at the separatrix of magnetic islands,

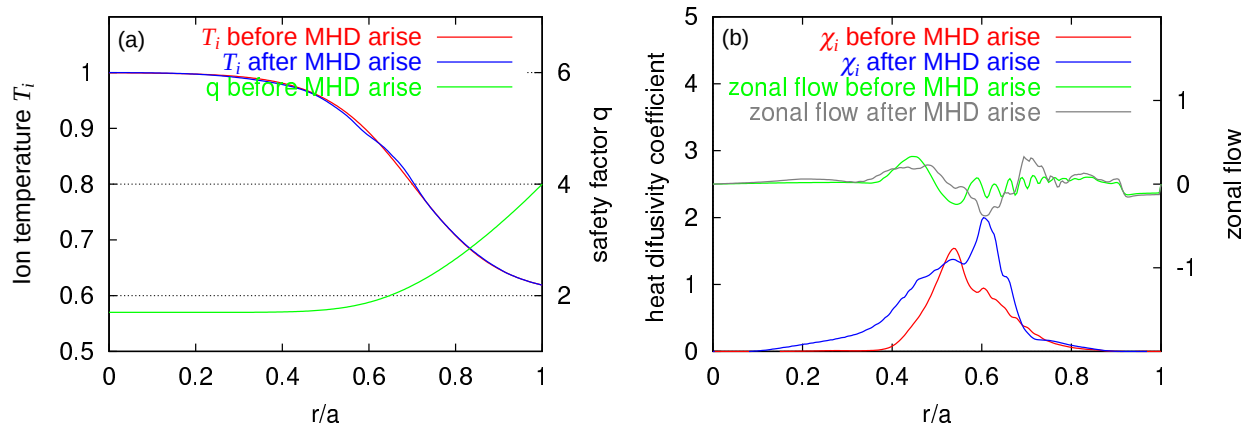

FIG. 6: *(a) Ion temperature profile T_i is flattened around magnetic islands that appears at rational surface of $q = 2$, $r_s/\tilde{a} = 0.65$ after the growth of tearing mode (macro-MHD). (b) Radial profiles of thermal diffusion coefficient and zonal flow. The thermal diffusivity increases around magnetic islands due to tearing mode.*

however, it is not clear whether the shear is strong at the separatrix.

4. Summary and Discussion

This is the first numerical simulation presenting anomalous transport due to coexistence of micro-turbulence with macro-MHD instability.

We have carried out three-dimensional simulation of a reduced set of two-fluid equations and have investigated effects of mutual interactions between micro-turbulence and macro-MHD instability on thermal transport. The initial equilibrium is unstable against kinetic ballooning mode (micro-instability) and tearing mode (macro-MHD instability), and the growth rate of former is larger than the latter. The micro-instability grows and a quasi-equilibrium including turbulence is formed at first, and it excites $(m, n) = (2, 1)$ mode through nonlinear mode coupling. We remark that this excitation of $(m, n) = (2, 1)$ mode by the turbulence is different from destabilization of tearing mode.

The $(m, n) = (2, 1)$ mode becomes the tearing mode (macro-MHD instability) and grows up in the quasi-equilibrium including the turbulence and zonal flow. The tearing mode affects the micro-turbulence and reduces the amplitude of it, in addition the energy of low toroidal mode number increases, and thus the energy spectrum of turbulence is changed. The reduction of micro-turbulence is not due to the flattening of temperature profile around magnetic islands because we have the reduction of micro-turbulence even if we fix the temperature profile as shown in Fig. 3. of Ref. [9]. After the appearance of tearing mode the ion temperature profile is flatten and the thermal diffusion coefficient χ_i increases around the magnetic islands due to tearing mode. We think that the macro-scale flow of tearing mode cooperates with small scale turbulent flow and produces large thermal diffusion. The zonal flow profile is altered by the appearance of tearing mode. It seems that the flow shear becomes strong around the magnetic island due to tearing mode.

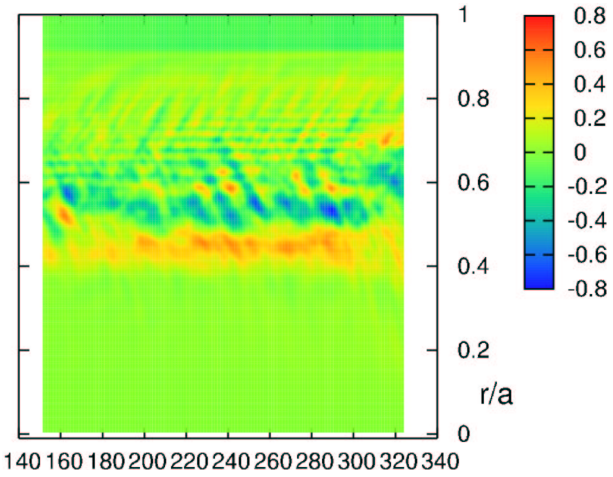

FIG. 7: *Time evolution of zonal flow profile. The profile changes around the location of magnetic islands,* $r_s/\tilde{a} = 0.65$*, after tearing mode appears at* $t = 290$*.*

Acknowledgments

The authors would like to thank Prof. Sudo for his encouragement. One of the authors A. I. is supported by the Japanese Ministry of Education, Culture, Sports, Science, and Technology, Grant No. 18760642.

References

[1] HORTON, W., Review of Modern Physics **71**, 735 (1999).
[2] TAKEJI, S., *et al.*, Nuclear Fusion **42**, 5 (2002).
[3] TANAKA, K., *et al.*, Nuclear Fusion **46**, 110 (2006).
[4] DIAMOND, P. H., *et al.*, Plasma Physics and Controlled Fusion **47**, R35 (2005).
[5] DIAMOND, P. H., *et al.*, Phys. Fluids **27**, 1449 (1984).
[6] ITOH, S. -I., *et al.*, Plasma Physics and Controlled Fusion **46**, 123 (2004).
[7] YAGI, M., *et al.*, Nuclear Fusion **45**, 900 (2005).
[8] McDEVITT, C. J. and DIAMOND, P. H., Phys. Plasmas **13**, 032302 (2006).
[9] ISHIZAWA, A. and NAKAJIMA, N., Physics of Plasmas, **14**, 040702 (2007).
[10] ISHIZAWA, A. and NAKAJIMA, N., Nuclear Fusion, **47**, 1540 (2007).
[11] ISHIZAWA, A. and NAKAJIMA, N., to appear in ”Theory of Fusion Plasmas”, AIP Conference Proceedings of Joint Varenna-Lausanne International Workshop (2008).
[12] ISHIZAWA, A. and NAKAJIMA, N., Physics of Plasmas, **15**, 084504 (2008).
[13] JOFFRIN, E. *et al.*, Nuclear Fusion **42**, 235 (2002).
[14] HAZELTINE, R. D., *et al.*, Phys. Fluids **30**, 320 (1987).
[15] SCOTT, B., Phys. Plasmas **7**, 1845 (2000).
[16] GARBET, X., *et al.*, Phys. Plasmas **8**, 2793 (2001).
[17] TANG, W. M., *et al.*, Nuclear Fusion **20**, 1439 (1980).
[18] FURTH, H. P., *et al.*, Phys. Fluids **6**, 459 (1963).